Journal of Visualization, Vol. 12, No. 1 (2009) 9-16

Regular Paper

Investigation of Piezoelectrically Generated Synthetic Jet Flow

Yang, A. S.*[1], Ro, J. J.*[2], Yang, M. T.*[2] and Chang, W. H.*[2]

*1 Department of Energy and Refrigerating Air-Conditioning Engineering, National Taipei University of Technology, Taipei 106, Taiwan. E-mail: asyang@ntut.edu.tw
*2 Department of Mechanical and Automation Engineering, Da-Yeh University, Changhua 51505, Taiwan. E-mail: jro001@mail.dyu.edu.tw

Received 22 October 2007
Revised 16 July 2008

Abstract: The purpose of this paper is to investigate the compressible turbulent synthetic jet flow characteristics of a dual diaphragm piezoelectric actuator. Experimentally, a flow visualization system was established to obtain the particle streak images scattered from 10-μm red fluorescent spheres for observing the synthetic jet flowfield produced by a dual diaphragm piezo actuator. The centerline velocity of the synthetic jet was also measured by using a hot-wire anemometry system. In the analysis, the computational approach adopted the transient three-dimensional conservation equations of mass and momentum with the moving boundary specified to represent the piezo diaphragm motion. The standard k-ε two-equation turbulent model was employed for turbulence closure. For the actuator operating at the frequency of 648 Hz, the particle streakline images in the cross-sectional plane visualized a turbulent jet flow pattern in the far-field area. The hot-wire anemometry data indicated that the measured centerline velocity of synthetic jets reached 3.8 m/s at y/d= 50. The predictions were compared with the visualized particle streak images and centerline velocity of the synthetic jet in order to validate the computer code. The numerical simulation revealed the time-periodic formation and advection of discrete vortex pairs. Caused by the outward movement of the piezo diaphragms, air near the orifice was entrained into the actuator cavity when the vortex pairs were sufficiently distant from the orifice.

Keywords : Synthetic jet flow, Piezoelectric actuators, Flow visualization system.

1. Introduction

The synthetic jet flow has the unique zero-mass-flux property. It has received increasing attention over the past several years because of its applications in active flow control (Cui and Agarwal, 2006; Tesar and Travnicek, 2005). Synthetic jet actuators can be also used to introduce unsteadiness into a larger-scale flow for augmenting the mixing and heat transfer processes (Beratlis and Smith, 2003; Chen, et al., 1999; Yang and Lee, 2006). In practice, a synthetic jet actuator consists of membranes located on end or side walls of a cavity with an orifice from where the fluid jet is discharged. The membrane is driven to oscillate using electrical, mechanical, magnetic or other measures. The inward motion of the membranes expels the fluid through the orifice, leading to generation of a vortex ring (or a vortex pair) at the edge of the orifice because of flow separation on the nozzle exit edge. When the membranes move outwards, the vortex ring travels away from the orifice and the fluid is entrained into the cavity with zero net mass flux achieved over each period of oscillation (Travnicek, et al., 2007; Ramesh, et al., 2006; Hargrave and Jarvis, 2006). Previously, steady or oscillating jets were delivered by compressed air or regulated blowers, which generally increased complexity and weight of the system (Seifert, et al, 1996; Smith and Swift, 2003). Various design and

fabrication concepts were applied to improve the performance of actuators with the objective of reaching simpler architecture and lower operational power. The piezoelectric actuator has recently become one of highly promising devices to produce synthetic jets through mechanical oscillations of piezoelectric diaphragms driven by a specific voltage waveform. The piezo-actuated diaphragms were utilized to generate volumetric displacement within a fluid-filled cavity for forming jets (Lee, et al., 2003; Smith, 1999; Gallas, et al., 2002). Meanwhile, substantial efforts were made to explore the flow structure of synthetic jets. The geometric configurations and operating conditions of piezo-actuators can affect the flow behavior of synthetic jets (Utturkar, 2002; Holman and Utturkar, 2005). Without net mass addition, synthetic jets were produced by oscillating flows having a zero mean velocity through an orifice (Cater and Soria, 1997; Crook, et al., 1999). It was clearly observed that the amplitude of oscillations was large enough to induce flow separation at the nozzle exit with the resulting vortex sheets rolled into vortex pairs advected away from the orifice under their own self-induced velocity (Fugal, et al., 2005). Furthermore, the progression of synthetic jets near the exit plane was mainly dominated by the time- periodic formation and advection of these vortex pairs. Jet flows eventually undergo the transition to turbulence, slow down and lose their coherence (Smith and Glezer, 1998). Most of the preceding research works investigated the jet flowfield driven by a single oscillating diaphragm. The present study aims at a characterization of the synthetic jet flow properties by using the particle streak imaging technique and a hot-wire anemometry system for a dual diaphragm piezo actuator. To conduct simulations of complex jet flow phenomena, a commercial computational fluid dynamics (CFD) package ACE+® was used as the framework for numerical calculations (ESI US R&D, 2004).

2. Experimental Approach

Figure 1 shows the schematic diagram of the overall experimental setup. A flow visualization system was established to obtain the particle streak images via 10-μm red fluorescent spheres for observing the synthetic jet flowfield formed by a dual-diaphragm piezoelectric actuator. The piezo diaphragms of the actuator were concurrently operated with a 180° phase differential at the same sinusoidal voltage and frequency from an electrical signal controller (Agilent 33120A Function Generator and TREK 601C Amplifier). A 5-W argon-ion laser (TSI INNOVA90, 532nm) with a plane-cylindrical lens was used as a light source to illuminate the jet in the cross-sectional plane. The streakline scattered from the fluorescent particles was photographed by a charge-coupled device (CCD) camera (SONY XC-HR57). The particle streak images were processed with an image acquisition board (DOMINO Harmony), displayed on the screen of a monitor, and then stored as a file in a computer.

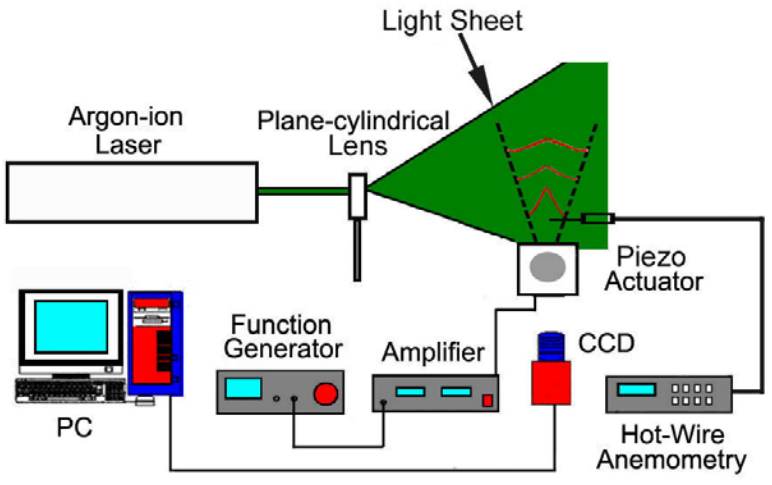

Fig. 1. Schematic diagram of the overall experimental setup

A hot-wire anemometry system (TSI 8495), operated in the constant-temperature mode, was also used to measure the jet centerline velocity. The single straight hot-wire probe was mounted on a two-axis steel extended contact bearing traversing gear (for position adjustment with a minimum resolution of 10 μm in the axial and transverse axes) and parallel to the length of the orifice exit. Since the probe was not sensitive to flow direction, measurements were limited to the areas of small transverse velocity. The axial velocity was acquired at the positions of 25 ~ 100 mm downstream of the actuator orifice center with 5 mm intervals. The hot wire was calibrated by an air flow velocity calibrator (TSI 8392 CERTIFIER®), and the accuracy in the measurements was ±1% over the course of this study.

Figure 2 depicts the picture of a dual diaphragm piezoelectric actuator. The piezo actuator had a housing in which a cylindrical cavity was enclosed by two brass diaphragms placed opposite each other. The cavity dimensions were 50 mm in diameter and 10 mm in depth, respectively. A disc-type piezoelectric diaphragm with 30-mm diameter and 0.15-mm thickness was attached to the center of the outside face of each brass diaphragm. The geometry of brass plate was 50 mm in diameter and 0.15 mm in thickness. During the tests, the controller was utilized to command the electrical signal for driving the piezo actuator. With an input sine waveform signal, the operating voltage and frequency were set at 60 V (peak to peak) and 648 Hz. A delay device could be also triggered by the controller to snatch the images of the jet flow from the actuator orifice by the CCD camera. Under actuation, a synthetic jet was issued from a 35.5 mm long by 0.5 mm wide orifice located on the top of the actuator. The measured results in terms of the overall shape and centerline velocity of the flow can enhance the understanding of the synthetic jet behavior and establish a useful database for model validation.

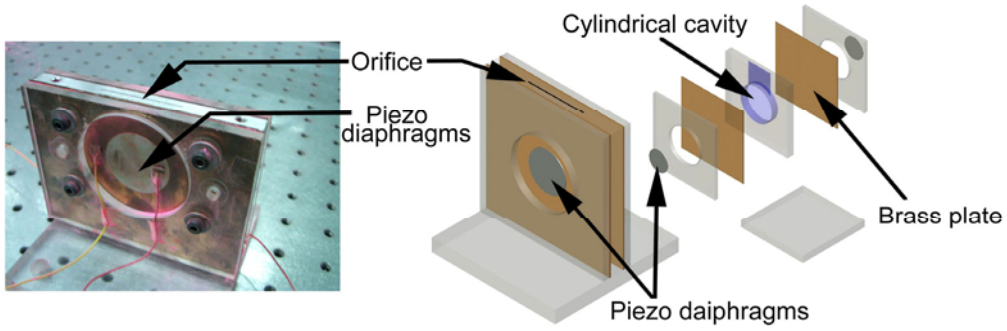

Fig. 2. Picture and assembly drawing of a dual diaphragm piezoelectric actuator

3. Theoretical Analysis

A theoretical analysis was performed using the CFD code ACE+® to explore the flow characteristics of synthetic jets. The model considered the transient, three-dimensional compressible turbulent flow with the governing equations written as below.

$$\frac{\partial \rho}{\partial t}+\frac{\partial(\rho u)}{\partial x}+\frac{\partial(\rho v)}{\partial y}+\frac{\partial(\rho w)}{\partial z}=0. \tag{1}$$

$$\frac{\partial}{\partial t}(\rho\vec{V})+\rho(\vec{V}\bullet\nabla)\vec{V}=-\nabla p+\rho\vec{g}+\frac{\partial}{\partial x_j}\left[\mu_{eff}\left(\frac{\partial u_i}{\partial x_j}+\frac{\partial u_j}{\partial x_i}\right)-\delta_{ij}\left(\frac{2}{3}\mu_{eff}\right)\nabla\bullet\vec{V}\right]. \tag{2}$$

The symbol u_i is the velocity component in the i axis with $\vec{V}$ as the velocity vector; whereas, p, ρ, and μ_{eff} correspond to the pressure, density, and effective viscosity (defined as the sum of laminar viscosity μ_l and turbulent viscosity μ_t), respectively. The term $\rho\vec{g}$ denotes the gravity force. The

standard k-ε two-equation turbulent model was adopted for turbulence closure.

$$\frac{\partial(\rho k)}{\partial t}+\nabla\bullet\rho\vec{V}k=\rho P-\rho\varepsilon+\frac{\partial}{\partial x}\left[\left(\mu_l+\frac{\mu_t}{\sigma_k}\right)\frac{\partial k}{\partial x}\right]+\frac{\partial}{\partial y}\left[\left(\mu_l+\frac{\mu_t}{\sigma_k}\right)\frac{\partial k}{\partial y}\right]+\frac{\partial}{\partial z}\left[\left(\mu_l+\frac{\mu_t}{\sigma_k}\right)\frac{\partial k}{\partial z}\right]. \quad (3)$$

$$\frac{\partial(\rho\varepsilon)}{\partial t}+\nabla\bullet\rho\vec{V}\varepsilon=C_{\varepsilon 1}\frac{\rho P\varepsilon}{k}-C_{\varepsilon 2}\frac{\rho\varepsilon^2}{k}+\frac{\partial}{\partial x}\left[\left(\mu_l+\frac{\mu_t}{\sigma_\varepsilon}\right)\frac{\partial\varepsilon}{\partial x}\right]+\frac{\partial}{\partial y}\left[\left(\mu_l+\frac{\mu_t}{\sigma_\varepsilon}\right)\frac{\partial\varepsilon}{\partial y}\right]+\frac{\partial}{\partial z}\left[\left(\mu+\frac{\mu_l}{\sigma_\varepsilon}\right)\frac{\partial\varepsilon}{\partial z}\right]. \quad (4)$$

Where μ_t is $C_\mu\rho k^2/\varepsilon$; k is the turbulent kinetic energy; ε is the turbulent energy dissipation rate; P is the turbulent kinetic energy production rate. The constants C_μ, $C_{\varepsilon 1}$, $C_{\varepsilon 2}$, σ_k and σ_ε were given as 0.09, 1.44, 1.92, 1.0 and 1.3, respectively. The above governing equations were discretized by the finite control volume method. For the convective terms, a second-order accurate central difference scheme was implemented with the adaptive damping for treating non-physical oscillations in the numerical solutions. A typical second-order accurate central difference scheme was utilized for evaluating the diffusion terms. The Crank-Nicolson scheme was applied to treat the unsteady term for providing the second-order accuracy in time. Additionally, the iterative semi-implicit method for pressure-linked equations consistent (SIMPLEC) numerical scheme was adopted for velocity-pressure coupling (Van Doormaal and Raithby, 1984). The calculation in the time evolution of jet formation was explicit and had an inherent stability requirement on the allowable timestep magnitude. In each numerical cell, the stability limit was restricted by the Courant-Friedrichs-Lewy (CFL) Number, defined as (the local velocity magnitude) × (the maximum timestep) / (the characteristic length of a local cell), which must satisfy the condition CFL< 1 via setting the automatic timestep option in the ACE+® code.

4. Results and Discussion

Numerical calculations were conducted with the computational fluid dynamics software ACE+® to validate the present theoretical model by comparing the predictions with experimental observations. Figure 3 illustrates the numerical grids of a full-size piezoelectric actuator for synthetic jet flow simulations. The mesh system mainly consisted of two structured sections. The cylindrical section in the lower part represents the air cavity inside the actuator, and the rectangular section in the upper part denotes the area outside the actuator for capturing the flow structure of a synthetic jet issued from an orifice sited on the top of the actuator. Finer grids were placed in the regions neighboring the exit of the orifice and near the moving and fixed wall boundaries with a smallest spacing of 47.8 μm for resolving steep variations of flow properties. The pressure in the surrounding area out of the orifice was 1 atm. The conditions of zero normal gradient of pressure and log-wall functions were imposed on the top surface of the actuator.

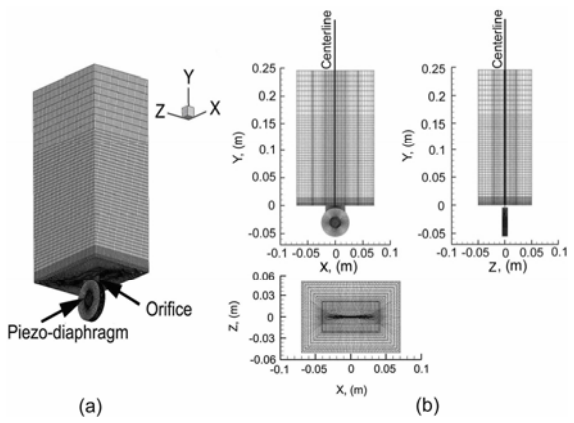

Fig. 3. Numerical grids of a full-size piezoelectric actuator for synthetic jet simulations (a) stereogram view, (b) top and side view

Under the applied driving voltage signal, the moving boundaries were specified to represent the motion of piezoelectric diaphragms [Tracute, et al., 2005]. The displacement was determined by the finite-element computer package ANSYS® with placing the values of piezoceramic material as Young's modulus of 9.1×10^{10} N/m^2, Poisson's ratio of 0.33, and density of 7900 kg/m^3, respectively. The fixed boundary condition of a diaphragm was used in the ANSYS transient analysis for the case filled with air from both sides. It revealed that the displacement responded as a sine wave having the same frequency of 648 Hz. The predicted piezo displacement from the ANSYS simulation was also verified by the experimental results of a Polytec scanning vibrometer (Polytec-MSV300®). It was found that the same maximum displacement, located at the center of the piezo diaphragm, was 90 μm outward and 90 μm inward (with the peak-to-peak amplitude of 0.18 mm) for both the ANSYS simulation and the measurement when operating at the identical condition. With air as the working fluid, the related density and viscosity are 1.18 kg/m^3 and 1.85×10^{-5} N-s/m^2 at the room temperature. Computations were also performed on total grids of 160760, 198888, and 256288 points at CFL= 0.5 and 0.25. To calculate each time-step, the normalized residual errors of flow variables (u, v, w, p, k and ε) converged to 10^{-5} with the mass conservation check within 0.5 %. The calculated results of the centerline velocity profiles at different grids and CFL values indicated that satisfactory grid independence could be attained using a mesh setup of 198888 grids with CFL= 0.5. A complete simulation for developing a stable synthetic jet typically necessitate s around 120 hours of central processing unit (CPU) time on a Pentium P4- 3.2GHz personal computer.

Figure 4 shows a comparison of the predictions with particle streak images of the synthetic jet in the mid cross-sectional plane at the frequency of 648 Hz. The overall flow pattern appeared to be a nearly fully developed turbulent air jet in the far-field region. It was also observed that the jet flow, exhausting into a quiescent environment from the piezo-actuated cavity, had a tendency to spread increasingly and mingle with the surrounding air. The jet structure then turned into a wake type of flow far downstream from the orifice. Generally, the predicted jet flow contour agreed well with the visualized image.

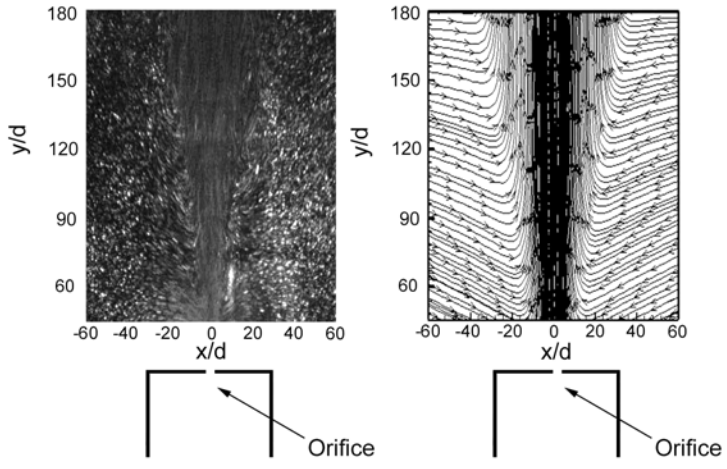

Fig. 4. Comparison of the predictions with visualized particle streak images of the synthetic jet in the mid cross-sectional plane at the frequency of 648 Hz

Figure 5 shows a comparison between the prediction and measured centerline velocities of the synthetic jet above the orifice. Here y is the distance from the orifice in the normal direction, and d is the width of the actuator orifice. Each data point stands for the mean value of five measured records with the error bars designated by $\pm3\sigma_{sd}$, where σ_{sd} is the standard deviation. The transverse component of velocity was very small relative to the axial component along the centerline of the jet. In the y/d ranging from 50 to 200, the hot-wire anemometry results revealed that the fluid always flowed away from the orifice with the value of ~3.8 m/s at y/d= 50. In the far field, the velocity also

decreased with streamwise distance. It was found that the maximum error between the predictions and the measured jet centerline velocities was within 3.82 %, indicating that the simulation code can predict synthetic jets with a reasonable accuracy.

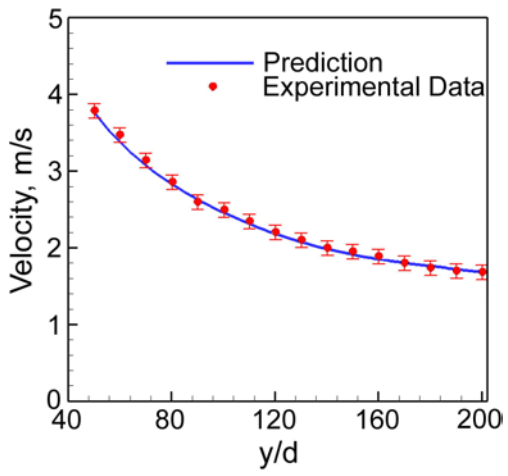

Fig. 5. Comparison between the prediction and measured jet centerline velocities above the orifice

Since the near-field flow properties of the jet were difficult to measure experimentally, a CFD simulation code was used to complete the understanding of the development process of synthetic jets. Figure 6 presents the calculated centerline velocity distributions of the synthetic jet flow over a full actuation cycle. Here u_{max} is the maximum axial velocity at the orifice. During the cycle, the calculated results indicated that the peak value of the axial velocity on the orifice reaches around 27 m/s (corresponding to a Reynolds number of 850 based on the width of the actuator orifice) at t/T= 1/4. The synthetic jet was essentially divided into two regions. In the region of y/d< 3.5, the predicted centerline velocity showed the unsteady flow behavior with $u(t)/u_{max}$ varying in a nearly sinusoidal waveform at y/d= 0.0. The averaged axial velocity and the net mass flux of the actuation cycle were zero at the exit plane of the orifice. As y/d> 3.5, the synthetic jet remained an upward fluctuating flow. The jet reached a steady axial velocity of 3.8 m/s with a variation of $(u(t)-u_{ave})/u_{ave}$ (u_{ave} defined as the time-averaged axial velocity) less than ± 3 % at y/d= 50. For the t/T period of 5/8－7/8, the negative axial velocities close to the orifice showed that the air was drawn into the actuator cavity due to the outward movement of the piezo diaphragms.

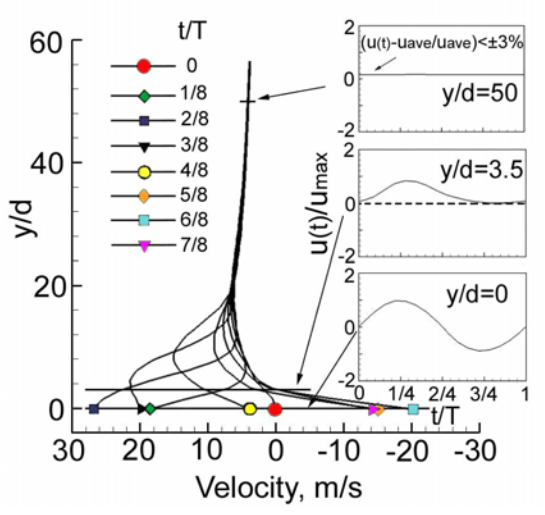

Fig. 6. Centerline velocity distributions of the synthetic jet flow over a full actuation cycle

Figure 7 shows the predicted streamline and axial velocity contours in a complete actuation cycle. The calculated results illustrated the time evolution of vortex pair for the synthetic jet formed by a dual-diaphragm piezoelectric actuator. In the early stage of t/T= 0－1/4, air was expelled via the orifice when the diaphragms moved inwards. Caused by the sudden contraction effect, the flow separation of the central jet (which occurred immediately in front of and downstream from the contraction channel) induced the rollup of a vortex pair at the edge of the orifice exit. Meanwhile, large eddies or vortices were also generated inside the actuator cavity when the air flow passed by the orifice. During the period of t/T from 3/8 to 1/2, the vortex pair was visibly formed and traveled upward in a progressive manner. For t/T> 5/8, the vortex pair proceeded advection away from the orifice under its own momentum. The vortex pair was sufficiently distant from the orifice so that it was not influenced by the entrainment of air into the cavity. It was also noted that those eddies in the actuator cavity disappeared and a fully reversed flow was developed due to fast retraction of the piezo diaphragms back to their original state.

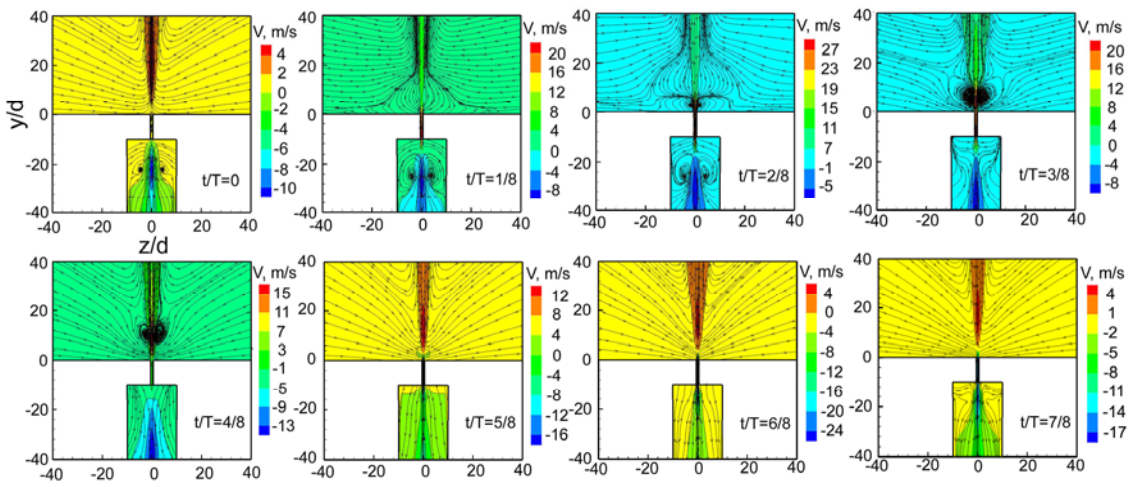

Fig. 7. Streamline and axial velocity contours in a full actuation cycle

5. Conclusion

A novel dual diaphragm piezoelectric actuator was successfully designed and fabricated to produce synthetic jets. Experimental and theoretical studies were performed to explore the formation process of the jet flow. In general, the progression of the synthetic jet can be separated into two zones. Near the exit plane of the orifice, the jet flow reveals the evolution behavior involving the time-periodic generation and advection of discrete vortex pairs. The vortex pair then undergoes the transition process to a nearly fully-developed turbulent jet flow in the far-field area. When the vortex pairs are far away from the orifice, the surrounding air is drawn into the actuator cavity due to the outward movement of the piezo diaphragms.

Acknowledgments

This study represents part of the results obtained under Contract NSC97-2221-E-027-023-MY2, sponsored by the National Science Council, Taiwan, ROC.

References

Beratlis, N. and Smith, M. K., Optimization of Synthetic Jet Cooling for Microelectronics Applications, Annual IEEE Semiconductor Thermal Measurement and Management Symposium, Inst. of Electrical and Electronics Engineers, (2003), 66–73.

Cui J. and Agarwal R. K., Three-Dimensional Computation of a Synthetic Jet in Quiescent Air, AIAA Journal, 44-12 (2006), 2857-2865.

Chen, Y., Liang, S., Aung, K., Glezer, A. and Jagoda, J., Enhanced Mixing in a Simulated Combustor Using Synthetic Jet Actuators. AIAA Journal, (1999), 99-0449.
Cater, J. E. and Soria, J., The Evolution of Round Zero-Net-Mass-Flux Jets, Journal of Fluid Mechanics, 472-01 (1997), 167-200.
Crook, A., Sadri, A. M. and Wood, N. J., The Development and Implementation of Synthetic Jets for the Control of Separated Flow, AIAA Journal, (1999), 99-3176.
ESI US R&D, CFD-ACE(U)® V2004 User's Manual, ESI-CFD Inc., Huntsville, AL, 2004. Web site: www.cfdrc.com.
Fugal, S. R., Smith, B. L. and Spall, R. E., Displacement Amplitude Scaling of a Two-Dimensional Synthetic Jet, Physics of Fluids, 17-4 (2005), 045103.
Gallas, Q., Mathew, J., Kasyap, A., Holman, R., Nishida, T., Carroll, B., Sheplak, M. and Cattafesta, L., Lumped Element Modeling of Piezoelectric-Driven Synthetic Jet Actuators, AIAA Journal, 41-2 (2003), 240-247.
Hargrave, G. K. and Jarvis, S., A Study of Premixed Propagating Flame Vortex Interaction, Journal of the Visualization, 9-2 (2006), 179-188.
Holman, R. and Utturkar, Y., Formation Criterion for Synthetic Jets, AIAA Journal, 43-10 (2005), 2110-2116.
Lee, C., Ha Q. P., Hong, G. and Mallinson, S. G., A Piezoelectrically Actuated Micro Synthetic Jet for Active Flow Control, Sensors and Actuators, 108-1 (2003), 168-174.
Ramesh, G., Venkatakrishnan, L. and Prabhu, A., PIV Studies of Large Scale Structures in the Near Field of Small Aspect Ratio Elliptic Jets, Journal of Visualization, 9-1 (2006), 23-30.
Seifert, A., Darabi, A. and Wygnanski, I., Delay of Airfoil Stall by Periodic Excitation, Journal of Aircraft, 33-4 (1996), 691-699.
Smith, B. L. and Swift, G. W., A Comparison Between Synthetic Jets and Continuous Jets, Experiments in Fluids, 34-4 (2003), 467–472.
Smith, B. L., Synthetic Jets and their Interaction with Adjacent Jets, PhD Thesis, Georgia Institute of Engineering, (2000), 3528.
Smith, B. L. and Glezer, A., The Formation and Evolution of Synthetic Jets, Physics of Fluids, 10-9 (1998), 2281–2297.
Tesar, V. and Travnicek, Z., Pulsating and Synthetic Impinging Jets, Journal of Visualization, 8-3 (2005), 201-208.
Tracute, V. C., Fedorchenko, Z. A. and Wang, A. B., Enhancement of Synthetic Jets by Means of an Integrated Valve-Less Fluid Pump. Part II. Numerical and Experimental Studies, Sensors and Actuators, 125-1 (2005), 50–58.
Travnicek, Z., Tesar, V. and Kordik, J., Performance of Synthetic Jet Actuators Based on Hybrid and Double-Acting Principles, Journal of Visualization, 11-3 (2008), 221-230.
Utturkar, Y., Mittal, R., Rampunggoon, P. and Cattafesta, L., Sensitivity of Synthetic Jets to the Design of the Jet Cavity, AIAA Journal, (2002), 0124.
Van Doormaal, J. P. and Raithby, G. D., Enhancements of the SIMPLE Method for Predicting Incompressible Fluid Flows, Numerical Heat Transfer, 7 (1984), 147-163.
Yang, C. J. and Lee, Y. H., Vortex Flow Patterns of a Heaving Foil, Journal of the Visualization, 9-1 (2006), 13-22.

Author Profile

An-Shik Yang: Dr. An-Shik Yang is an Associate Professor of Department of Energy and Refrigerating Air-Conditioning Engineering at National Taipei University of Technology (NTUT), in Taiwan. His research interests are in the areas of micro-fluidic design, multiphase fluid dynamics, and heat transfer. Prior to joining NTUT in fall 2007, Dr. Yang was a faculty member of Department of Mechanical and Automation Engineering at Da-Yeh University in Taiwan from 2000 to 2007. He received his B.S. (1982) and M.S. (1984) degrees from National Tsing-Hua University in Taiwan, and Ph.D. (1993) degree from Pennsylvania State University in USA. All three degrees are in Mechanical Engineering with an emphasis in the thermo-fluid sciences.

Jeng-Jong Ro: Dr. Jeng-Jong Ro joins the Department of Mechanical and Automation Engineering at Da-Yeh University as an associate professor on August 2000. Before he joined Da-Yeh University, He was a faculty member of Aerospace Engineering at Old Dominium University, Virginia during 1997 to 2000. Dr. Ro earned Ph.D. and M.S. degrees in Mechanical Engineering from Catholic University of America, Washington D.C. in 1990 and 1993. His research interests include active and passive control of structural vibration and radiated noise using smart materials, the design and analysis of piezoelectric synthetic jet actuators and the investigation of piezoelectric harvesting system.

Ming-Tang Yang: Mr. Ming-Tang Yang received his M.S. degree in Mechanical and Automation Engineering form Da-Yeh University, Taiwan in 2007. He joined NAK SEALING TECHNOLOGIES CORPORATION as a R&D Engineer in 2007. His research interests are system analysis, simulation and experiment flow dynamics.

Wei-Han Chang: Mr. Wei-Han Chang is currently a graduate student in Mechanical and Automation Engineering of Da-Yeh University in Taiwan. His M.S. thesis topic is Flow Behavior Study of Synthetic Jets. His research interests are computer-aided engineering analysis, experiment flow dynamics, and power MEMS.